Original Article

Efficacy and preliminary dose studies of ultrasound-guided sclerotherapy with lauromacrogol for the treatment of implanted hepatic tumors in rabbits

Shilong Wang[1], Ming Yin[1], Zhichao Xia[2]

[1]Department of Ultrasound, The Affiliated Taizhou People's Hospital of Nanjing Medical University, Taizhou, China; [2]Department of Clinical and Research, Shenzhen Mindray Biomedical Electronics Co., Ltd., Shenzhen, China

Contributions: (I) Conception and design: M Yin; (II) Administrative support: Z Xia; (III) Provision of study materials or patients: S Wang; (IV) Collection and assembly of data: S Wang; (V) Data analysis and interpretation: M Yin, S Wang; (VI) Manuscript writing: All authors; (VII) Final approval of manuscript: All authors.

Correspondence to: Ming Yin. Department of Ultrasound, The Affiliated Taizhou People's Hospital of Nanjing Medical University, Taizhou, China. Email: yinriyue@sina.com.

Background: To study the curative effect of sclerotherapy with lauromacrogol on a rabbit VX2 implanted liver tumor model, the effect of ultrasound-guided sclerotherapy with different doses of lauromacrogol in the treatment of the rabbit VX2 implanted liver tumor model and the degree of damage to the surrounding liver tissue was compared and observed. The relationship between the sclerosing effect and drug dose of lauromacrogol in the treatment of liver cancer is preliminarily discussed.

Methods: Thirty rabbit models of liver cancer were randomly divided into 5 groups. Control Group A was injected with normal saline, control Group B was injected with absolute ethanol, experimental Group C was injected with lauromacrogol (Z =2.885D); the injection volume in experimental Group D was 1.5-fold higher than that in Group C; and the injection volume in experimental Group E was 2-fold higher than that in Group C. Changes in tumor volume were followed up by ultrasound before and 7 and 14 days after the operation; contrast-enhanced ultrasonography was used to measure the volume of the ablation area and volume rate. For pathological anatomy, hematoxylin and eosin (H&E) staining were used to observe tumor cell necrosis and the degree of damage to surrounding normal liver cells. The expression levels of the apoptosis-related protein cleaved-caspase 3 and the cell proliferation antigen Ki67 were examined by immunohistochemistry.

Results: The volumes in Groups A and C increased significantly. The volumes in Groups B, D, and E remained the same or slightly expanded, tumor growth in the three groups was significantly inhibited after sclerotherapy. Contrast-enhanced ultrasonography showed that the ablation volume and ablation volume rate in Groups B, D, and E were similar. Group C were smaller than those in the other treatment groups. Large coagulative necrotic foci were observed in the central area of tumors in Groups B, D, and E.

Conclusions: The experiment demonstrates that lauromacrogol can inhibit tumor growth in the rabbit VX2 tumor model and cause VX2 tumor cell apoptosis. The sclerosing effect of the 1.5-fold amount of lauromacrogol is equivalent to that of absolute ethanol, with little effect on normal liver tissue.

Keywords: Ultrasound guided; lauromacrogol; sclerotherapy; liver tumor

Submitted Nov 06, 2022. Accepted for publication Feb 08, 2023. Published online Feb 23, 2023.
doi: 10.21037/jgo-23-16
View this article at: https://dx.doi.org/10.21037/jgo-23-16

Introduction

According to the 2019 China Guidelines for the Diagnosis and Treatment of Primary Liver Cancer (1), surgery and liver transplantation are the preferred treatment methods for hepatocellular carcinoma (HCC), but for patients who have lost the opportunity for surgery, local ablation therapy has become the second choice. Radiofrequency ablation (RFA), microwave ablation (MWA), and percutaneous ethanol injection (PEI) are the most commonly used local ablation methods in China.

PEI is a technique in which absolute ethanol is injected into liver cancer. Absolute ethanol causes tumor cell dehydration, degeneration, and necrosis with microvascular thrombosis, resulting in tumor ischemia and destruction and ultimately tumor tissue necrosis. The advantages of PEI are that it is economical and affordable, causes few complications after ablation for liver cancer in high-risk locations, and is simple and reproducible.

However, the disadvantage of absolute ethanol is that it causes severe abdominal pain and high fever, and its use is impossible for those allergic to alcohol. Therefore, it has become a new research direction to find a new type of chemical ablation drug to replace absolute ethanol.

Lauromacrogol, a new type of sclerosing agent in clinical practice, is mainly used for sclerotherapy of varicose veins and liver and kidney cysts. Its effect is comparable to that of absolute ethanol. Lauromacrogol has been confirmed to have a significant killing effect on liver cancer cells and to inhibit the growth of liver cancer cells in a dose-dependent manner in *in vitro* experiments using liver cancer cell lines (2,3).

A previous study has reported that the sclerosing effect of lauromacrogol is comparable to that of absolute ethanol in subcutaneous liver tumor experiments of sclerotic mice (4). However, no research has explored the application of lauromacrogol alone to liver cancer, and the effect on tumor sclerosis in the liver environment is unknown. Furthermore, no studies on the doses of lauromacrogol are available.

Therefore, this experiment simulated the liver cancer environment to explore the therapeutic effect of lauromacrogol on VX2 liver cancer in rabbits compared with the treatment effect of absolute ethanol and then explored the therapeutic effect of different doses of lauromacrogol on cirrhotic liver cancer, as well as the effect on liver cancer tissue and the surrounding liver tissue. This study provides a theoretical basis for the application of lauromacrogol in the clinical treatment of liver cancer in the future. We present the following article in accordance with the ARRIVE reporting checklist (available at https://jgo.amegroups.com/article/view/10.21037/jgo-23-16/rc).

Highlight box

Key findings

- This study provides a theoretical basis for the application of lauromacrogol in the clinical treatment of liver cancer in the future.

What is known and what is new?

- Absolute ethanol can inhibit the proliferation and division of cancer cells.
- High doses of lauromacrogol is comparable to the effect of absolute ethanol.

What is the implication, and what should change now?

- A previous study has reported that the sclerosing effect of lauromacrogol is comparable to that of absolute ethanol in subcutaneous liver tumor experiments of sclerotic mice. This experiment simulated the liver cancer environment to explore the therapeutic effect of lauromacrogol on VX2 liver cancer in rabbits compared with the treatment effect of absolute ethanol and then explored the therapeutic effect of different doses of lauromacrogol on cirrhotic liver cancer. as well as the effect on liver cancer tissue and the surrounding liver tissue.

Methods

Materials

Experimental animals: thirty liver tumor-bearing rabbits, male or female, weighing 2.0–3.0 kg were provided by the Animal Laboratory of Jiangsu Zhenlin Biotechnology Co., Ltd. The animal experiments in this study were approved by the Ethics Committee of Taizhou Jianyouda Biomedical Technology Co., Ltd. and followed the national guidelines for the care and use of animals. A protocol was prepared before the study without registration.

Drugs: Anesthetics: Zoletil, lauromacrogol, SonoVue, etc.

Main instruments: Color Doppler ultrasound: Mindray M9, frequency 4–12 MHz.

Experimental grouping

Thirty liver tumor-bearing rabbits were randomly divided into 5 groups, and the injection dose was calculated using the regression equation Z=2.885D for the reference of absolute ethanol injection, D is the maximum diameter of the tumor (cm), Z is the injection dose (mL) (5). The

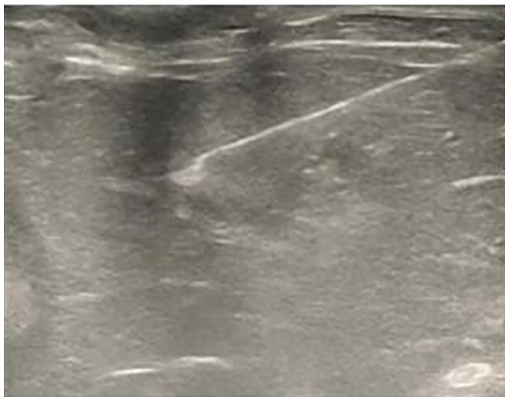

Figure 1 Ultrasound-guided therapy.

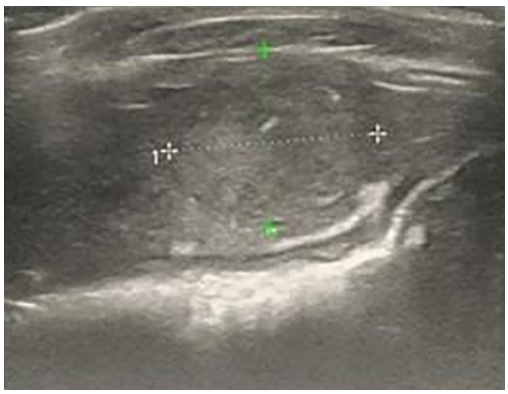

Figure 2 Preoperative two-dimensional ultrasound measurement of tumor size.

corresponding dose of sclerosant was injected into tumor in each model group, and the control Group A was sham treatment Group (6 rabbits): each rabbit was injected with normal saline, the injection volume was based on the regression equation Z=2.885D; control Group B (6 rabbits): each rabbit was injected with absolute ethanol, and the injection volume was based on the regression equation Z=2.885D; experimental Group C (6 rabbits): each rabbit tumor was injected with lauromacrogol, and the injection volume was based on the regression equation Z=2.885D; experimental Group D (6 rabbits): the injection volume was based on regression equation Z=2.885D×1.5; the experimental Group E (6 animals): the injection volume was based on the regression equation Z=2.885DX×2.

Ultrasound-guided sclerotherapy

The feeding was stopped for experimental rabbits 24 hours before the operation, and rabbits were weighed before the operation. Zoletil anesthesia was intravenously injected via marginal ear vein. The maximum diameter of liver cancer of each VX2 tumor rabbit was measured by grayscale ultrasound before operation, and the corresponding doses of normal saline, absolute ethanol and lauromacrogol were prepared. Routine iodophor disinfection was performed, and drapes were prepared. Under the guidance of ultrasound, the needle tip was punctured into the tumor. Under the guide of ultrasound, normal saline was injected into Group A, absolute ethanol was injected into Group B, and 1-fold, 1.5-fold and 2-fold volumes of lauromacrogol were injected into Groups C, D, and E, respectively. Multipoint puncture was implemented, and the degree of drug diffusion in the tumor was observed until the drug diffused to the entire tumor (*Figure 1*). On the 7th day after the operation, normal saline, absolute ethanol and lauromacrogol were injected again in the same way. The major element which affects the efficacy of treatment is the loss of drugs. Therefore, the injection of drugs gradually moves from the root of the tumor to the shallow layer of the tumor. Injection should be multi-point injection, injection, multiple directions and rotation can be slowly lift needle handle, make the average distribution of the drug in tumors (6).

Specific detection methods

Two-dimensional grayscale ultrasonography was carried out before operation and 7 and 14 days after operation to observe the changes in the tumor surface echoic halo, internal echo, internal and peripheral blood flow and to calculate the tumor volume. Selecting the follow-up time (nal grayscale ultrasonography was carried out) is according to (4) the ultrasound follow-up time. The maximum diameter (a), minimum diameter (b), and width diameter (c) of tumor before and after the treatment were measured based on the methods in the publications. The tumor volume was calculated according to the formula V=a×b×c/2 mm^3 calculation (4) (*Figure 2*).

Measurement of the volume of the ablation zone by contrast-enhanced ultrasound: 14 days after the operation, contrast-enhanced ultrasonography was performed to measure the length (L), width (W), and thickness (D) of the tumor ablation zone in each rabbit. The volume of the ablation zone was measured based on V=π/6×L×W×D (7). The tumor ablation rate was calculated as follows: tumor ablation rate = volume of ablation area/tumor volume.

Changes in aspartate transaminase (AST) in liver

function: blood was drawn from the ear vein of experimental rabbits before operation and 1, 3, and 7 days after operation, and the changes in ALT (Alanine aminotransferase) in liver function of experimental rabbits were observed.

Pathological examination

(I) H&E staining: after the 14th day of the experiment, the experimental rabbits were sacrificed, the liver was removed by laparotomy, and the tumor and surrounding tissues were excised and fixed with 10% formaldehyde. The routine paraffin-embedded sections were stained with H&E, and the pathological changes in the normal liver tissue in and around the tumor were observed under a microscope.

(II) Effects of lauromacrogol on apoptosis and proliferation of VX2 HCC cells were evaluated using immunohistochemical examination: immunohistochemical examination was conducted to measure the expression levels of apoptosis protein cleaved-caspase 3 and cell proliferation antigen Ki67 to explore whether lauromacrogol can induce tumor cell apoptosis and inhibit tumor cell division.

(III) Pathological section preparation and H&E staining steps.

Evaluation of results

Comparison of tumor volume and size between groups. Taking the tumor volume change of the absolute ethanol group as a reference, the tumor volume changes in groups treated with different doses of lauromacrogol were compared between each group, and the effect of sclerotherapy in each group was evaluated.

To observe tumor development by contrast-enhanced ultrasound, we measured the ablation volume under the contrast-enhanced state, compared the difference between the ablation volume and ablation volume rate between groups, and evaluated the ablation effect of each group.

Immunohistochemical results. The staining results were judged by two independent pathologists using a double-blind method. Cleaved-caspase 3 was positively expressed in the cell membrane and cytoplasm, and the positive cells were brown granules (3). Under 400× magnification, 6 fields of view were randomly selected for each slice, and positive cell staining was judged (A): <5% (0 points), 5–25% (1 point), 26–50% (2 points), >50% (3 points). Positive intensity (B): without staining or light yellow uniform with the background (0 points), light tan (1 point), tan (2 points), brown (3 points). A×B was used to score; 0–1 was negative (–), 2–3 was weakly positive (+), 4–6 was positive (++), and 7–9 was strongly positive (+++), and the area of apoptosis and necrosis was estimated under high magnification. The positive expression of the Ki67 protein molecule was located in the nucleus, and the brown–yellow positive signal of Ki67 overlapped with the blue-stained nucleus, which appeared tan or even dark brown (8). Under the microscope at 400× magnification, 5 fields of view were randomly selected to calculate the positive cell ratio. Ki67 detection took 14% as the cutoff value, less than 14% as low expression, and ≥14% as high expression.

Statistical analysis

All measurement data are expressed as the mean ± standard deviation and were analyzed using the SPSS 25.0 statistical software package. The tumor size at each time point and the intergroup and intragroup changes in ALT were analyzed by two-way repeated measures analysis of variance; the intergroup comparison of the ablation volume was performed by one-way analysis of variance, with $P<0.05$ indicating significant differences and $P<0.01$ indicating very significant differences.

Results

Grayscale ultrasonography and color Doppler ultrasonography: ultrasonography was performed before operation and 7 and 14 days after operation. The tumor body before operation was shown as a hypoechoic mass with a regular round or oval shape, and some tumors were accompanied by a hypoechoic halo; Color Doppler flow imaging (CDFI) revealed annular and linear blood flow signals in and around the tumor (*Figure 3*). Ultrasound examination was performed on the 14th day after the operation. In addition to the increase in volume, irregular anechoic areas appeared in individual tumors in Group A, indicating liquefaction and necrosis during tumor growth. Groups B, D, and E showed uneven distribution of echoes inside the tumor. CDFI indicated that the internal blood flow signal had disappeared, and no blood flow signal or star-like blood flow signal was noted (*Figure 4*). In Group C, the tumor was enlarged, the internal echo became thicker, and uneven strong echo mass shadows were observed. CDFI showed linear and surrounding blood flow signals.

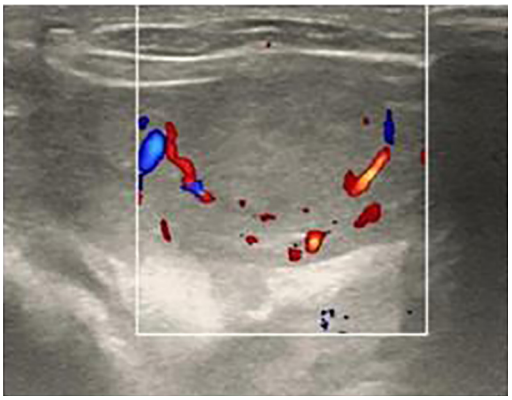

Figure 3 Preoperative CDFI showing a peripheral annular blood flow signal. CDFI, color Doppler flow imaging.

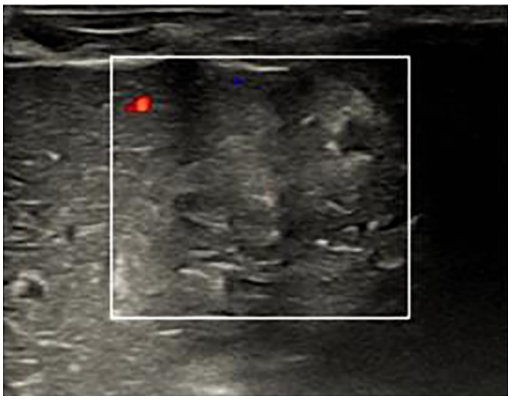

Figure 4 Postoperative CDFI showing a decreased blood flow signal. CDFI, color Doppler flow imaging.

Table 1 Tumor volume in each group before and after treatment (Data are presented as mean ± standard deviation)

Group	Tumor size (mm^3)		
	Original volume	Volume after 7 days	Volume after 14 days
Saline group	1,278.86±258.75	2,477.17±393.2	6,605.73±1,271.02[b,c,d,e]
Absolute ethanol group	1,392.61±330.68	1,446.12±437.67	1,476.97±464.98[a,b]
1-fold lauromacrogol group	1,201.50±259.78	2,021.91±544.52	2,766.61±705.57[a,c,d,e]
1.5-fold lauromacrogol group	1,214.76±303.45	1,206.06±345.49	1,258.04±292.59[a,b]
2-fold lauromacrogol group	1,286.72±277.52	1,319.1±303.19	1,342.42±318.11[a,b]

[a], indicates a statistical difference compared with the saline group (P<0.05); [b], indicates a statistical difference compared with the 1-fold lauromacrogol group (P<0.05); [c], indicates statistical difference compared with the absolute ethanol group (P<0.05); [d], indicates statistical difference compared with the 1.5-fold lauromacrogol group (P<0.05); [e], indicates statistical difference compared with the 2-fold lauromacrogol group (P<0.05).

Changes in tumor volume: after two treatments for 14 days, the preoperative tumor volumes in the 5 groups of VX2 tumor-bearing rabbits were compared between the groups, which revealed no significant difference (P=0.794). The volumes in Group A and Group C increased significantly from (1,278.86±258.75) mm^3 and (1,201.50±259.78) mm^3 to (6,605.73±1,271.02) mm^3 and (2,766.61±705.57) mm^3, respectively; Group A was the sham treatment group, and the tumor volume was in a state of natural growth. The tumor volume in Group C was similar to that in the lauromacrogol group, and tumor growth was inhibited to a certain extent. The difference between the two groups was considered significant at P<0.05. The tumor volumes in Groups B, D, and E grew from their original sizes of (1,392.61±330.68) mm^3, (1,214.76±303.45) mm^3, and (1,286.72±277.52) mm^3 to (1,476.97±464.98) mm^3, (1,258.04±292.59) mm^3, and (1,342.42±318.11) mm^3, respectively. Generally, the tumor volumes in the three groups receiving sclerotherapy remained the same or were slightly expanded, and tumor growth in the three groups was significantly inhibited after sclerotherapy, which was significantly different from observations in sham treatment Group A, the 1-fold lauromacrogol group (P<0.05). No significant difference was found among the three groups (B, D, and E), and the sclerosis effects were comparable (*Table 1*, *Figures 5*,*6*).

Contrast-enhanced ultrasonography manifestations: preoperative contrast-enhanced ultrasonography indicated that the tumor was in a state of rapid enhancement in the arterial phase, and it was in a state of rapid decline in the venous phase and the delayed phase. The performance is a typical "fast in and fast out" state (*Figure 7A*).

On the 14th day after the operation, variable filling defects were noted in the arterial phase of contrast-enhanced ultrasonography for treatment groups. In the absolute

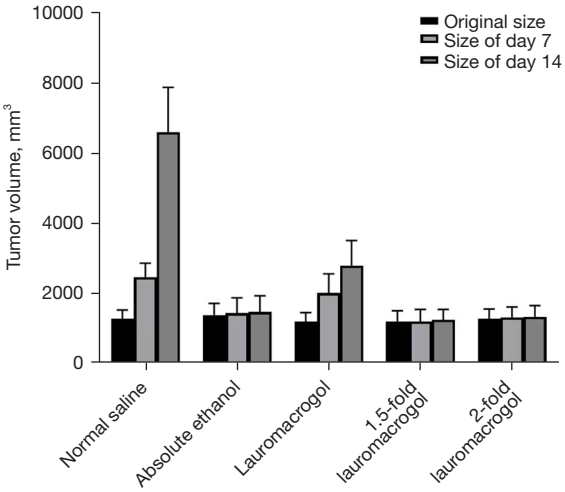

Figure 5 Tumor volume growth in each group before and after treatment.

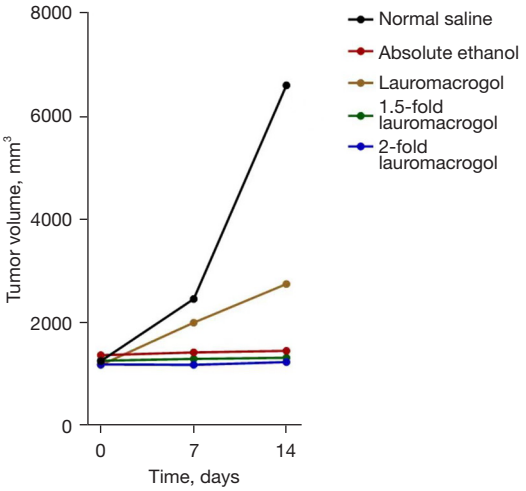

Figure 6 Tumor growth trends in each group.

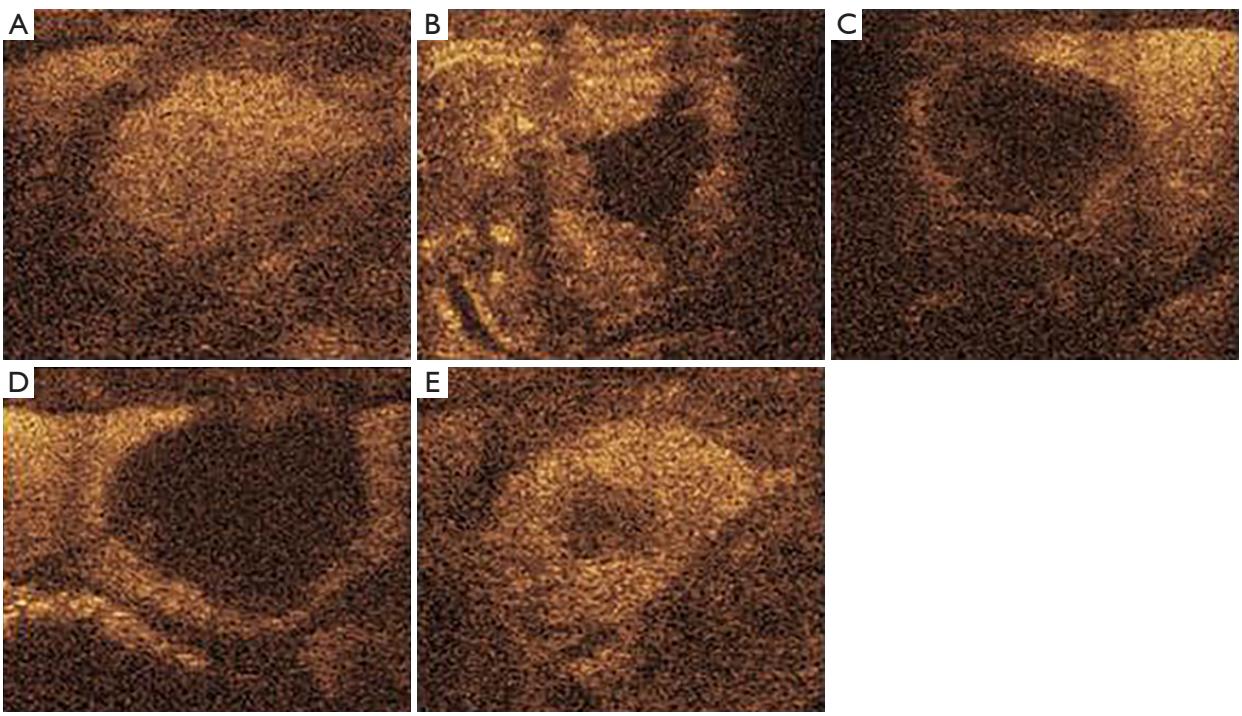

Figure 7 Contrast-enhanced ultrasound performance. (A) Saline group contrast-enhanced ultrasound images of the tumor. (B) Contrast-enhanced ultrasound images of Ablation zone in the absolute ethanol group. (C) Contrast-enhanced ultrasound images of Ablation zone in the 1.5-fold lauromacrogol group. (D) Contrast-enhanced ultrasound images of Ablation zone in the 2-fold lauromacrogol group. (E) Contrast-enhanced ultrasound images of Ablation zone in the 1-fold lauromacrogol group.

ethanol group, most tumors in the arterial phase had filling defect areas with relatively irregular margins, with a size of 1,042.29±320.91 mm^3, and a ring-shaped enhanced perfusion zone around them, which was considered residual cancer tissue (*Figure 7B*). In the 1.5-fold lauromacrogol group and the 2-fold lauromacrogol group, the tumor

Table 2 Ablation volumes and ablation volume rates

Group	Ablation area (mm^3)	Ablation volume rate
Saline group	–	–
Absolute ethanol group	1,042.29±320.91[a]	0.7068±0.0419[b]
1-fold lauromacrogol group	511.9±125.05	0.1972±0.081
1.5-fold lauromacrogol group	845.82±177.92[a]	0.6608±0.0355[b]
2-fold lauromacrogol group	905.54±161.33[a]	0.6826±0.0549[b]
F value	6.904	113.302
P value	0.02	0.00

Data are presented as mean ± standard deviation. [a], the ablation volume ratio between the groups is greater than 0.05, with no significant difference; and [b], the ablation volume ratio between the groups is greater than 0.05, with no significant difference.

Table 3 ALT changes before and after treatment

Group	ALT (U/L)			
	Before the operation	1 day after the operation	3 days after the operation	7 days after the operation
Saline group	46.17±5.91	48.83±3.19	48.17±4.62	47.50±3.99[b]
Absolute ethanol group	48±3.74	84±6.87	62.83±4.36	44.33±4.76[a,b]
1-fold lauromacrogol group	47.17±10.80	78.17±3.25	63.17±4.22	46.33±6.50[a,b]
1.5-fold lauromacrogol group	46.5±4.93	80±6.72	64.17±3.76	50.67±7.28[a,b]
2-fold lauromacrogol group	50.67±7.94	113.83±11.25	78.5±7.56	52±4.73[a,b]

Data are presented as mean ± standard deviation. [a], statistically different from the saline group with P<0.05; [b], statistically different from the 2-fold lauromacrogol group with P<0.05. ALT, alanine aminotransferase.

showed a relatively regular filling defect area with sizes of (845.82±177.92) mm^3 and (905.54±161.33) mm^3, respectively, in the arterial phase, and strongly enhanced residual cancer tissue was observed at the tumor edge (*Figure 7C*,*7D*). Ultrasonography of the lauromacrogol group revealed a small filling defect area in the arterial phase, with a size of 511.90±125.05 mm^3, with a large amount of residual perfusion around it (*Figure 7E*). The ablation volumes in the absolute ethanol group, 1.5-fold lauromacrogol group, and 2-fold lauromacrogol group were compared, with no significant difference (P>0.05). When comparing the 1-fold lauromacrogol group, absolute ethanol group, 1.5-fold lauromacrogol group, and the 2-fold lauromacrogol group, a significant difference (P<0.05) was identified among them. At the same time, the ablation volume rates of Groups B, D, and E were 0.7068±.0419, 0.6608±0.0355, and 0.6826±0.0549, respectively, with no significant difference between groups (P>0.05). The ablation volume rate in Group C was 0.1972±0.081, and compared with those in Groups B, D, and E, a significant difference was identified (P<0.05), indicating that the ablation effects in Groups B, D, and E were similar to and better than those in Group C (*Table 2*).

Changes in ALT: the sham treatment Group A was used as the reference: (46.17±5.91), (48.83±3.19), (48.17±4.62), and (47.50±3.99) U/L at 4 time points after the first sclerotherapy session, which were almost unchanged. The ALT levels of the experimental rabbits in Groups B, C, D, and E all increased on the first day after sclerotherapy, began to fall on the third day, and returned to normal levels on the seventh day. The difference between Group A and the treatment group was significant (P<0.05); compared with those in Groups B, C, and D, the ALT value increased significantly (113.83±11.25 U/L) on the first day after the operation in the 2-fold lauromacrogol group (P<0.05), suggesting that after sclerotherapy, transient liver function damage occurs but resolves within a short period. The 2-fold dose of lauromacrogol causes more significant transient liver damage (*Table 3*, *Figure 8*).

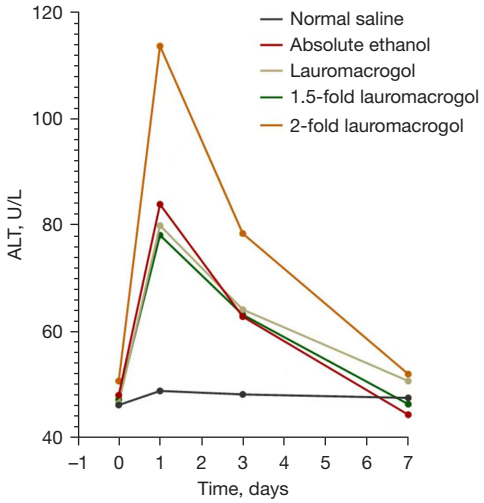

Figure 8 Change in ALT in the experimental rabbits. ALT, alanine aminotransferase.

H&E results

Normal saline Group A: the tumors were poorly differentiated, arranged in nests, with round and oval nuclei and visible mitoses. The liver capsule was invaded, scattered focal necrosis around the tumor was evident, no obvious fibrous tissue hyperplasia around the cancer nests could be observed, and hydropic degeneration of surrounding hepatocytes and perihepatic metastatic nodules could be observed (*Figure 9*).

Absolute ethanol group, 1.5-fold lauromacrogol group, 2-fold lauromacrogol group: the tumor was poorly differentiated, arranged in nests, with round or oval nuclei and large coagulative necrosis foci in the central part of the tumor, nuclei showed obvious pyknosis, ranging from approximately one-half to three-fourths of their original size, scattered focal necrosis were evident in the tumor margin, and fibrous tissue hyperplasia and inflammatory cell infiltration were observed around the cancer nest; peritumoral liver tissue had different degrees of fibrosis, inflammatory response, multinucleated giant cell response, and calcium deposition in the foci. The 2-fold lauromacrogol dose caused more damage to the peritumoral liver tissue. In addition to the severe fibrosis and inflammation in the normal peritumoral liver tissue, local coagulative necrosis of the surrounding liver tissue was evident (*Figure 10A-10E*).

In the 1-fold lauromacrogol group, limited flaky coagulative necrosis was seen inside the tumor, the range was approximately one-fourth, and fibrous tissue proliferation

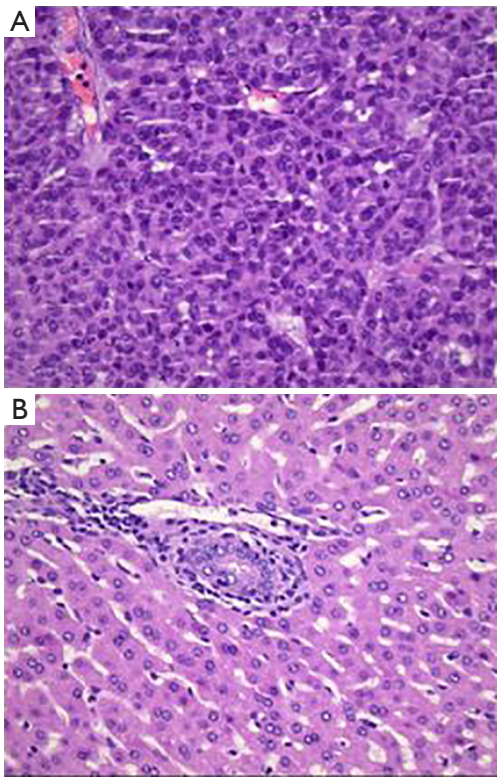

Figure 9 H&E staining in the saline group. (A) H&E staining of liver cancer tissue in the saline group, the tumors were poorly differentiated, arranged in nests, with round and oval nuclei and visible mitoses. (×400). (B) H&E staining of normal liver tissue around the tumor, hydropic degeneration of surrounding hepatocytes and perihepatic metastatic nodules could be observed (×400). H&E, hematoxylin and eosin.

and a small amount of inflammatory cell infiltration were seen around the cancer nest. No significant damage to the surrounding liver tissue was evident, and again, perihepatic metastatic nodal foci were observed (*Figure 10F*).

Immunohistochemical results

The cleaved-caspase 3 was expressed in a small amount in the VX2 tumor cells in the normal saline group, and the apoptotic necrosis area was approximately 15% of the tumor area. The expression of cleaved-caspase 3 was upregulated to different degrees in the absolute ethanol group and lauromacrogol group. The expression of cleaved-caspase 3 was upregulated in the absolute ethanol group, and the apoptotic and necrosis area was approximately 55%. The expression of cleaved caspase 3 was slightly upregulated

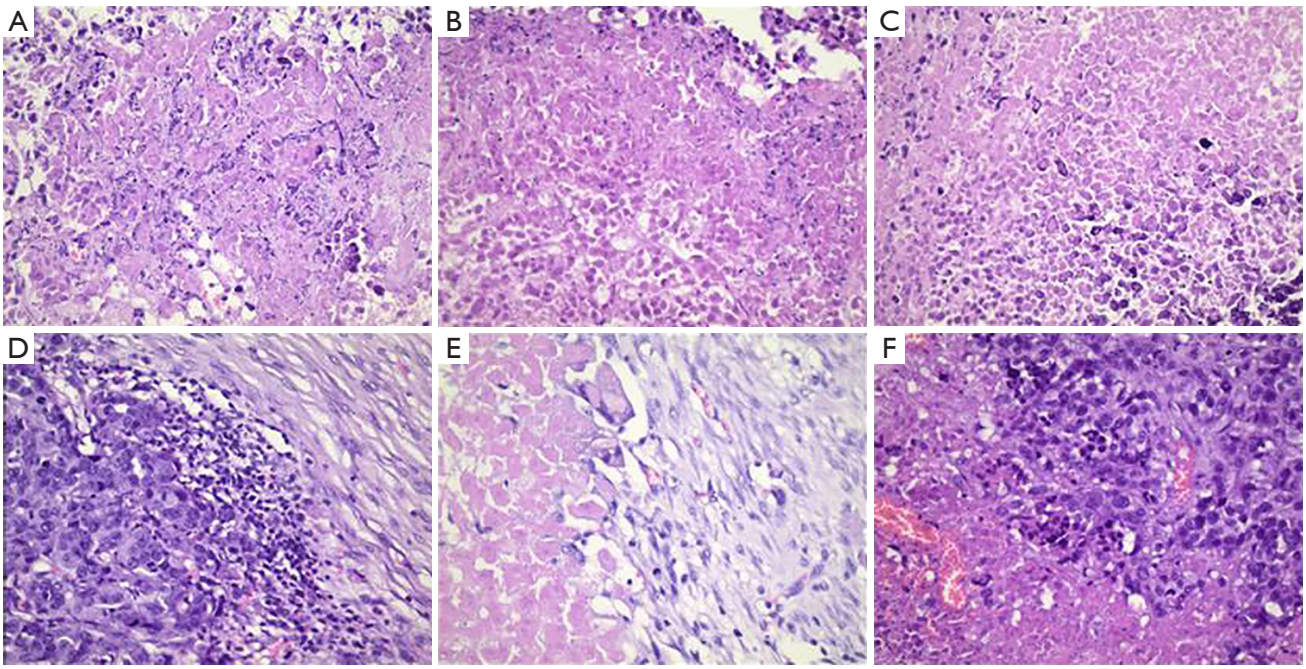

Figure 10 (A) H&E staining of a central necrotic tumor in the absolute ethanol group, coagulative necrosis foci in the central part of the tumor (×400). (B) H&E staining of a central necrotic tumor in the 1.5-fold lauromacrogol group coagulative necrosis foci in the central part of the tumor (×400). (C) H&E staining of a central necrotic tumor in the 2-fold lauromacrogol group, coagulative necrosis foci in the central part of the tumor (×400). (D) H&E staining of inflammation and fibrous tissue proliferation around the tumor (×400). (E) H&E staining of necrotic peritumoral liver tissue, local coagulative necrosis of the surrounding liver tissue was evident (×400). (F) H&E staining of scattered necrotic tumor tissues in the 1-fold lauromacrogol group (×400). H&E, hematoxylin and eosin.

in the 1-fold lauromacrogol group, and the apoptotic and necrosis area was approximately 35%. The apoptotic and necrosis area was approximately 45% in the 1.5-fold lauromacrogol group, the expression signal was the most evident in the 2-fold lauromacrogol group, and the area of apoptosis and necrosis was approximately 60% (*Figure 11*).

The Ki67 protein expression signal in VX2 tumor cells in the saline group was the most significant, while in the drug treatment group, the Ki67 protein expression signal in the 1-fold lauromacrogol group was slightly attenuated, but it was still highly expressed. The levels of Ki67 protein in the absolute ethanol group, 1.5-fold lauromacrogol group, and 2-fold lauromacrogol group were lower (*Figure 12*).

Discussion

Sclerotherapy of rabbit VX2 liver cancer with lauromacrogol

Lauromacrogol is mainly used for sclerotherapy of esophagogastric varices and lower extremity varicose veins. Later, it was clinically used as a sclerosing agent in some diseases and had an excellent effect, such as Ultrasound-guided polidocanol for symptomatic giant hepatic cystr syasound-guided sclerosant injection for cesarean scar pregnancy; low-dose sclerotherapy with lauromacrogol in the treatment of infantile Hemangiomas; the efficacy of laparoscopic lauromacrogol sclerotherapy in the treatment of simple hepatic cystsh (9-12). Lauromacrogol has been confirmed to have a significant killing effect on liver cancer cells in *in vitro* experiments on liver cancer cell lines and inhibit the growth of liver cancer cells in a dose-dependent manner. Yin *et al.* applied lauromacrogol and absolute ethanol in a study of subcutaneous liver cancer tumor sclerotherapy in mice and concluded that lauromacrogol can effectively kill liver cancer cells and inhibit the growth of liver cancer, and its effect is equivalent to that of absolute ethanol (4). Yang *et al.* applied lauromacrogol to ablate normal liver tissue. The pathological results demonstrated that lauromacrogol can destroy the normal structure of hepatic lobules, dehydrate necrotic liver cells, cause nuclei to undergo pyknosis and dissolution, and cause

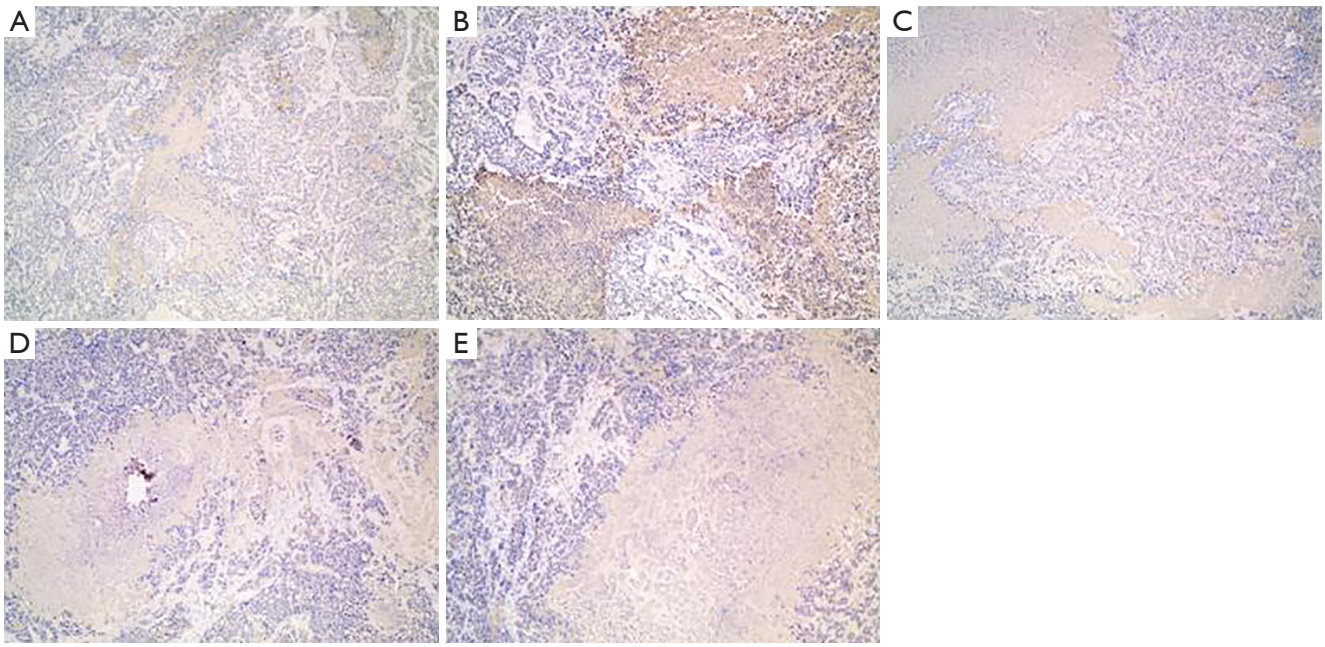

Figure 11 Use EnVision two-step dyeing expression of cleaved-caspase 3 protein (EnVision). (A) Low expression of cleaved-caspase 3 protein in the saline group (×40). (B) High expression of cleaved-caspase 3 protein in the absolute ethanol group (×40). (C) Increased expression of cleaved-caspase 3 protein in the 1-fold lauromacrogol group (×40). (D) High expression of cleaved-caspase 3 protein in the 1.5-fold lauromacrogol group (×40). (E) High expression of cleaved-caspase 3 protein in the 2-fold lauromacrogol group (×40).

eosinophilic changes in the cytoplasm and a large amount of inflammatory cell infiltration. In addition, a large amount of red blood cell accumulation and necrosis can be observed in the liver sinusoids, central veins, and interlobular veins (5).

This experiment used the VX2 liver transplant tumor model. The VX2 tumor cell line is actually a viral cell line called Shope, which is a squamous cell carcinoma derived from papilloma in rabbit skin. After 72 rounds of transplantation and passage, the strain was officially established and named VX2 (7). Due to similar pathological characteristics between rabbit and human HCC, this model has become an ideal animal model for clinical research on liver cancer.

After two sclerotherapy sessions for 14 days, two-dimensional grayscale ultrasound was used to observe tumor volume changes in real time. The 1.5-fold lauromacrogol group, 2-fold lauromacrogol group, and absolute ethanol group had the same therapeutic effect—inhibition of tumor growth. However, the tumor volume was not significantly reduced, for the following reasons: (I) when lauromacrogol and absolute ethanol act in the tumor body, fibrous separation occurs in the tumor body, which reduces the area affected by the drug, resulting in incomplete sclerotherapy, and the residual cancer tissue continues to grow, which reduces treatment efficiency. (II) Some tumors are close to hepatic blood vessels, and the drugs are therefore taken away by the bloodstream. (III) The observation period was short, and the tissue in the tumor necrosis area was not completely absorbed. Pathology revealed fibrosis in and around the cancer nest, which also confirmed that the fibrous septum would be formed after the direct effect of lauromacrogol on the tumor. Therefore, the effect of *in vivo* sclerotherapy with lauromacrogol should be similar to that of absolute ethanol, requiring multiple courses of treatment and multiple points of treatment such that the drug can be diffused to the entire tumor as much as possible.

Preoperative contrast-enhanced ultrasonography indicated that the VX2 tumor was similar to human HCC, supplying blood to the hepatic artery and showing typical "fast in and fast out" signs. Postoperative contrast-enhanced ultrasonography can help the operator determine the necrotic area of tumor tissue for chemical ablation, evaluate the treatment effect, and determine whether residual cancer tissue is present to provide a therapeutic direction for the next tumor ablation session. Postoperative contrast-enhanced ultrasonography revealed that both lauromacrogol

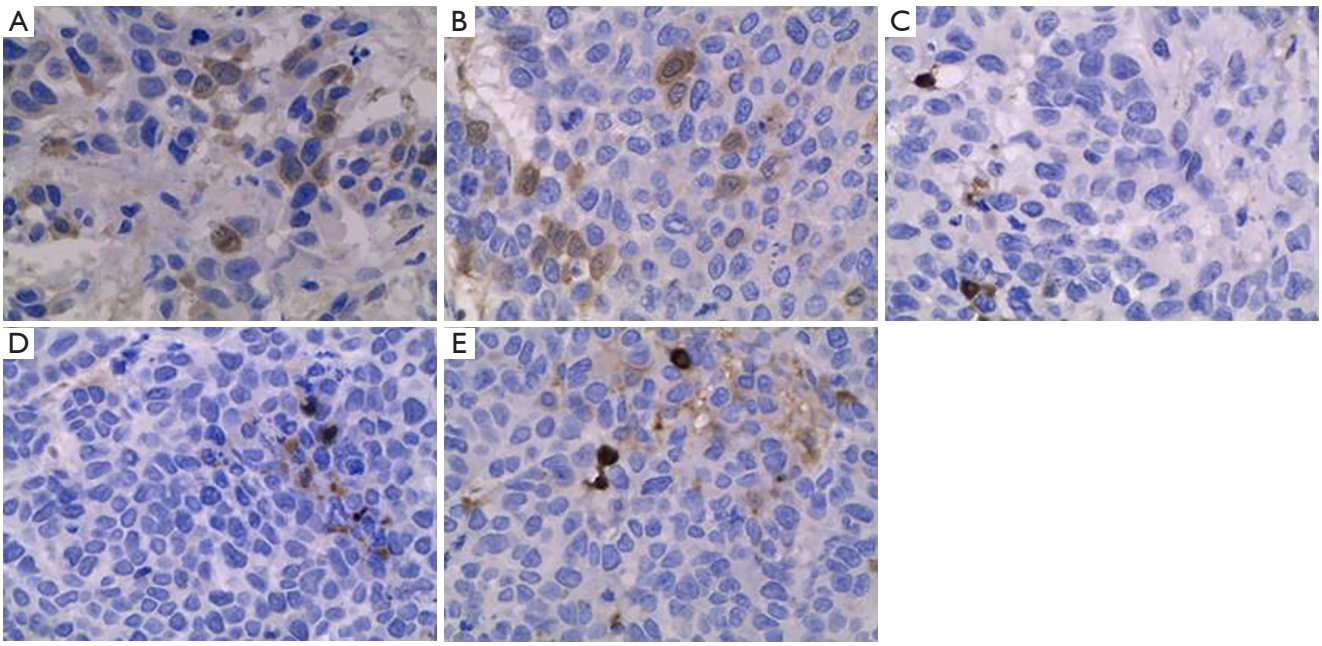

Figure 12 Use EnVision two-step dyeing expression of Ki67 protein. (A) High expression of Ki67 protein in the saline group (×400). (B) High expression of Ki67 protein in the 1-fold lauromacrogol group (×400). (C) Low expression of Ki67 protein in the absolute ethanol group (×400). (D) Low expression of Ki67 protein in the 1.5-fold lauromacrogol group (×400). (E) Low expression of Ki67 protein in the 2-fold lauromacrogol group (×400).

and absolute ethanol killed tumor tissue and destroyed its internal blood supply, and the contrast revealed a contrast-filled defect in the ablation area. Contrast-enhanced ultrasonography demonstrated that lauromacrogol had an ablation effect on VX2, but some incomplete ablation and residual cancer tissue next to it were evident. Compared with those in the high-dose lauromacrogol group and the absolute ethanol group, the volume of the ablation zone in the 1-fold lauromacrogol group was significantly reduced, indicating that a 1-fold dose of lauromacrogol had a poor sclerosis effect on the tumor, and the dose was not sufficient. The ablation rate was low and insufficient to inhibit tumor growth, allowing most of the cancerous tissue to remain.

At present, absolute ethanol is used for liver cancer ablation in clinical practice in two ways: (I) calculation of the dose according to the formula of $V=4/3\pi(r+0.5)^3$ (V is the total injection dose, and r is the radius of the lesion)(13); and (II) calculation of the dose according to the regression equation Y=2.885x (tumor diameter ≤5), Y=1.805x (tumor diameter >5), where X is the maximum diameter of the tumor (cm), and Y is the amount of ethanol injected (mL). In this experiment, the injection dose of absolute ethanol was used as the reference, and the injection dose of lauromacrogol was preliminarily explored. The 1.5-fold lauromacrogol group, the 2-fold lauromacrogol group, and the absolute ethanol group had the same therapeutic effect in terms of inhibition of the growth of the tumor volume and the size of the tumor ablation area. However, the pathological results and the liver function (ALT) of the experimental rabbits indicated that the damage to the normal liver tissue around the cancer in the 2-fold lauromacrogol group was significantly greater than that in the other groups, and a large amount of peritumoral liver tissue died. The extent of the ALT change also demonstrated that the 2-fold lauromacrogol dose was too high, causing a more pronounced transient elevation and increasing the burden on the liver, which is contrary to the principle of treatment. In contrast, 1.5-fold lauromacrogol causes less damage to the liver by ensuring the effect of sclerotherapy, which can provide a reference for the dose of lauromacrogol in sclerotherapy for liver cancer in the future.

The effect of lauromacrogol on apoptosis and proliferation of VX2 liver cancer cells

In this experiment, the levels of the cleaved-caspase

3 and the Ki67 in VX2 tumor cells were measured by immunohistochemistry (14-16). Lauromacrogol has been demonstrated to upregulate the expression of cleaved-caspase 3 in VX2 tumors and induce cell apoptosis. Apoptosis may be due to the ability of lauromacrogol to activate a certain signaling pathway within the cell that produces endothelial cell death by activating cellular calcium signaling and nitric oxide pathways. Therefore, cell death may occur through two mechanisms: one is direct destruction of the cell membrane, and the other is activation of the apoptosis pathway and cell necrosis induction. The related pathway mechanism of cell apoptosis should be further explored. The VX2 tumor in the normal saline group, as a pseudotreatment group, showed high expression of Ki67, which is consistent with the pathological results. The pathological findings demonstrated that the VX2 tumor was poorly differentiated squamous carcinoma and had developed liver metastases. Large doses of lauromacrogol can downregulate the expression of Ki67 in VX2 tumor cells and inhibit cell proliferation. However, Ki67 expression remained high in the low-dose group, possibly due to the stimulation of tumor cell proliferation caused by low-dose drug stimulation, which induced the proliferation and division of tumor cells.

Conclusions

In conclusion, animal experiments have demonstrated that lauromacrogol can inhibit the growth VX2 tumors in rabbits and cause apoptosis of VX2 tumor cells. High doses of lauromacrogol can inhibit the proliferation and division of cancer cells, which is comparable to the effect of absolute ethanol. The sclerosing effect of the 1.5-fold lauromacrogol dose is equivalent to that of absolute ethanol, with little effect on the normal liver tissue around the liver, which can be used as a preliminary reference for the lauromacrogol dose for sclerotherapy for the treatment of liver cancer.

Acknowledgments

Funding: None.

Footnote

Reporting Checklist: The authors have completed the ARRIVE reporting checklist. Available at https://jgo.amegroups.com/article/view/10.21037/jgo-23-16/rc

Data Sharing Statement: Available at https://jgo.amegroups.com/article/view/10.21037/jgo-23-16/dss

Peer Review File: Available at https://jgo.amegroups.com/article/view/10.21037/jgo-23-16/prf

Conflicts of Interest: All authors have completed the ICMJE uniform disclosure form (available at https://jgo.amegroups.com/article/view/10.21037/jgo-23-16/coif). Dr. ZX is from Shenzhen Mindray Biomedical Electronics Co., Ltd. The other authors have no conflicts of interest.

Ethical Statement: The authors are accountable for all aspects of the work in ensuring that questions related to the accuracy or integrity of any part of the work are appropriately investigated and resolved. The animal experiments in this study were approved by the Ethics Committee of Taizhou Jianyouda Biomedical Technology Co., Ltd. and followed the national guidelines for the care and use of animals.

References

1. Medical Administration of the National Health Care Commission of the People's Republic of China. Standardization for diagnosis and treatment of primary hepatic carcinom (2019 edition). Chinese Journal of Practical Surgery 2020;40:121-38.
2. Hu Z, Zhang Z, Li J, et al. The migration and proliferation effects of Lauromacrogol on hepatocellular carcinoma cell in vitro. Acta Universitatis Medicinalis Anhui 2013;48:772-5.
3. Sun J, Liu Y, Li Y, et al. The Expression of the Caspase-9 in Rabbit Liver VX2 Tumor-remnant Tissues after Radio-frequency Ablation Treatment. Chinese Journal of Ultrasound in Medicine 2010;26:8-10.
4. Yin M, Wang Z, Xiao W. Ultrasound-guided injection of lauromacrogol into liver cancer: an experimental study in

nude mouse models. Journal of Interventional Radiology 2016;25:530-3.
5. Yang J, Ding Y, Qiao W, Synergistic effects of focused ultrasound enhanced lauromacrogol in ablation of rabbit liver:an experimental study. Journal of Clinical Ultrasound in Medicine 2019;21:721-4.
6. Song XL, Shang GC. Poly cinnamyl alcohol injection and anhydrous ethanol ultrasonic guided therapy. Liver hemangioma curative effect comparison. J Intervent Radiol 2017;26.
7. Liu X, Ren L, Su G, et al. Establishment and characterization of a rabbit tumor cell line VX2. Chinese Journal of Pathology 2005;34:661-3.
8. Ghosh A, M N, Padmanabha N, et al. Assessment of p16 and Ki67 Immunohistochemistry Expression in Squamous Intraepithelial Lesion with Cytohistomorphological Correlation. Iran J Pathol 2020;15:268-73.
9. Eso Y, Shimizu H, Takai A, et al. Ultrasound-guided polidocanol foam sclerotherapy for symptomatic giant hepatic cyst: A single-center experience. Hepatol Res 2022;52:557-65.
10. Zhu L, Gao J, Yang X, et al. The novel use of lauromacrogol: A respective study of ultrasound-guided sclerosant injection for cesarean scar pregnancy. J Obstet Gynaecol Res 2022;48:140-5.
11. Wang C, Sun J, Guo L, et al. Low-dose sclerotherapy with lauromacrogol in the treatment of infantile hemangiomas: A retrospective analysis of 368 cases. Front Oncol 2022;12:1014465.
12. Xu S, Rao M, Pu Y, et al. The efficacy of laparoscopic lauromacrogol sclerotherapy in the treatment of simple hepatic cysts located in posterior segments: a refined surgical approach. Ann Palliat Med 2020;9:3462-71.
13. Nakai M, Sato M, Yamada K, et al. Percutaneous hot ethanol injection therapy (PHEIT) for hepatocellular carcinoma. Gan To Kagaku Ryoho 2001;28:1633-7.
14. O'Donovan N, Crown J, Stunell H, et al. Caspase 3 in breast cancer. Clin Cancer Res 2003;9:738-42.
15. Crowley LC, Waterhouse NJ. Detecting Cleaved Caspase-3 in Apoptotic Cells by Flow Cytometry. Cold Spring Harb Protoc 2016;2016.
16. Yang C, Zhang J, Ding M, et al. Ki67 targeted strategies for cancer therapy. Clin Transl Oncol 2018;20:570-5.

Cite this article as: Wang S, Yin M, Xia Z. Efficacy and preliminary dose studies of ultrasound-guided sclerotherapy with lauromacrogol for the treatment of implanted hepatic tumors in rabbits. J Gastrointest Oncol 2023;14(1):265-277. doi: 10.21037/jgo-23-16

